ANALYSIS OF FILTRATION MECHANISM OF CROSSFLOW UPWARD AND DOWNWARD ULTRAFILTRATION

EIJI IRITANI, TOMOHISA HAYASHI AND TOSHIRO MURASE
Department of Chemical Engineering, Nagoya University, Nagoya 464-01

Key Words: Membrane Separation, Ultrafiltration, Crossflow Filtration, Solid Liquid Separation, Gel Cake, Shear Stress, Upward Filtration, Downward Filtration, Proteinaceous Solution, Colloidal Solution

The filtration characteristics of crossflow ultrafiltration are studied for two types of solutes, a protein (BSA) and a colloid (silica sol), under constant-pressure conditions. It is shown that the time variation of the filtration rate coincides with that of dead-end ultrafiltration until the filtration rate drops to a certain value, and that the gel-cake is easily swept away at a relatively small crossflow velocity. Effects of the crossflow velocity, the filtration pressure and the solute concentration on the dynamically balanced filtration rate are explained by considering the balance between the "particulate" solutes accumulating on the gel-cake surface and those to be swept away by the shear force due to crossflow at steady state. It was also found that the dynamically balanced filtration rate in crossflow upward ultrafiltration coincides with that in dead-end upward ultrafiltration under conditions below the critical shear stress $\tau_{w\cdot c}$, whereas it is in accord with that in crossflow downward ultrafiltration above $\tau_{w\cdot c}$.

Introduction

Ultrafiltration has a broad variety of applications in the fields of biotechnology, biomedicine, and food and beverage processing, because the solution can be processed economically, even on a large scale, without the use of high temperatures. The most serious operational constraint in the use of ultrafiltration systems is that of membrane fouling. In ultrafiltration the gel-cake, which provides an extremely large hydraulic resistance to permeate compared with microfiltration and cake filtration, forms on the membrane surface. This gel-cake brings about the membrane fouling, which can be observed as a progressive reduction in filtration rate (flux). Therefore, crossflow filtration, in which the fluid being filtered flows parallel to the membrane surface, is useful in limiting the formation of gel-cake. Although a number of models[2,7,9,15,17,18,25-28] of crossflow ultrafiltration have been proposed, the mechanism of separation is still a matter of controversy. It may be essential to examine various filtration characteristics of the gel-cake deposited on the membrane surface in detail in order to clarify the real mechanism of crossflow ultrafiltration.

In the previous papers,[10,11] unstirred dead-end ultrafiltration experiments were conducted under constant-pressure conditions, using a batchwise filter which had a sudden reduction in its filtration area in order to measure the characteristic values of the gel-cake. It has been demonstrated experimentally that the thickness of a gel-cake which has an extremely large average specific filtration resistance builds up with filtration time, thereby decreasing the filtration rate and the drag force on the solutes, and that the solutes are packed loosely except for those adjacent to the membrane because of the high compressibility of the gel-cake.

Therefore, it is expected that the gel-cake in ultrafiltration may be easily swept away owing to its highly porous structure and the small drag force on the solutes compared with that in microfiltration or conventional filtration. In the present work, crossflow ultrafiltration experiments are conducted at relatively small crossflow velocity, and the effects of experimental conditions on the filtration characteristics are examined. In addition, the experimental results of crossflow upward ultrafiltration,[6] in which the filtrate flow is opposite in direction to gravity, are compared with those of conventional crossflow downward ultrafiltration.

1. Experimental Apparatus and Procedure

The experimental setup is schematically shown in **Fig. 1**. All ultrafiltration experiments are performed in a flat-channel system with a length of 9 cm, a width of 2 cm and a height of 6 mm. From a reservoir the solution is pumped through the filter chamber with a crossflow velocity in the range from 0 to 9.3 cm/s and then back to the reservoir by a peristaltic pump. Constant-pressure ultrafiltration experiments are conducted by introducing nitrogen gas into the free space of the reservoir under transmembrane pressures of 25 to 147 kPa, controlled by a reducing valve. The

* Received June 5, 1990. Correspondence concerning this article should be addressed to T. Murase. T. Hayashi is now with Eisai Co., Ltd., Ibaragi 314-02.

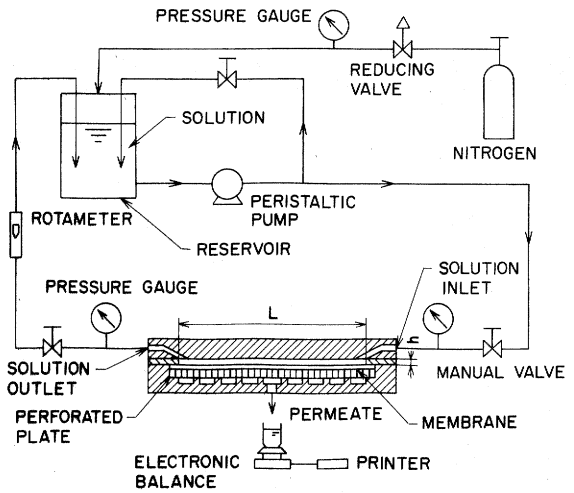

Fig. 1. Schematic diagram of experimental apparatus

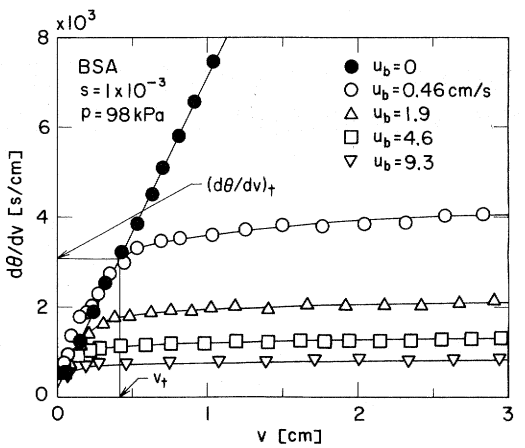

Fig. 2. Effects of crossflow velocity on filtration rate for BSA solution

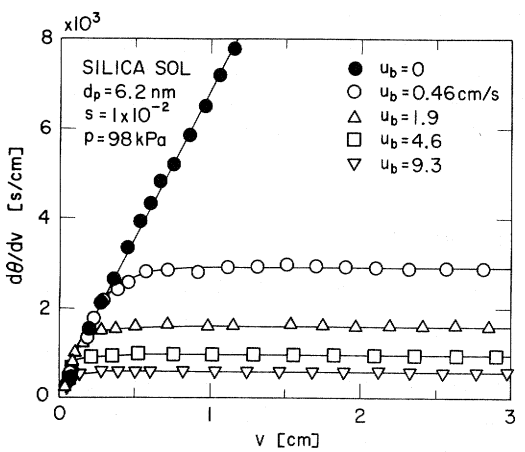

Fig. 3. Effects of crossflow velocity on filtration rate for silica sol

permeate is measured versus time by an electronic balance. For comparison, crossflow upward ultrafiltration experiments are also conducted.

Solutes used in this study are bovine serum albumine (BSA) (Fraction V, Katayama Chemical Ind.) with a molecular weight of about 69,000, and silica sol (Snowtex, Nissan Chemical Ind.) with mean diameters ranging from 6.2 to 48.3 nm. The pH values of these solutions are about 5.0 (isoionic/isoelectric points) for BSA and 9.9 for silica sol. Polyethersulfone membranes (OM030, Filtron) with nominal molecular weight cut-off of 30,000 are used for all the experiments to ensure almost complete rejection for the solutes used.

2. Experimental Results and Discussion

2.1 Factors influencing crossflow downward ultrafiltration rate

Typical data for ultrafiltration are plotted as the reciprocal filtration rate ($d\theta/dv$) versus the filtrate volume v per unit membrane area (well known as the Ruth plot[19,20] in conventional cake filtration) for BSA solution in **Fig. 2** and for silica sol in **Fig. 3**. For dead-end ultrafiltration in the absence of crossflow, the plots are virtually linear in the same manner as for cake filtration. Thus cake filtration equations[19,20] can be applied to such "solutions" as BSA as well as to suspensions of particulates.[21] The most striking feature for crossflow ultrafiltration is that the plot shows a linear relationship in accordance with that of dead-end ultrafiltration (crossflow velocity $u_b = 0$) until the filtration rate drops to a critical value $(dv/d\theta)_t$ which increases with u_b. This means that in this period the same gel-cake as that of dead-end ultrafiltration forms on the membrane surface. The obvious inference from this result is that sweeping of the gel-cake along the membrane surface or diffusion of the solute from the membrane does not occur during this initial stage. As the filtration process continues, however, the filtration rate decreases gradually and as a result the drag force on the solutes which constitute the gel-cake decreases. Consequently, the gel-cake begins to be swept away, and then the filtration rate tends to approach a plateau or dynamically balanced value. This quasi-steady rate increases with u_b. In ultrafiltration of silica sol and BSA solutions the gel-cake can be easily swept away by a relatively small crossflow velocity as shown in the figure, while a rather large crossflow velocity is required in order to maintain a constant filtration rate in microfiltration for polymethyl methacrylate (PMMA) and yeast suspensions.[12,14] The difference in crossflow velocities required in ultrafiltration and in microfiltration presumably occurs because in ultrafiltration most of the gel-cake except for that part of the vicinity of the membrane is in a wet and loose condition. This would be expected from the inference that in ultrafiltration the solid compressive pressure is very small in most of the gel-cake because the high compressibility of the gel-cake yields a marked change in the compressive pressure near the membrane.[23,24]

Figure 4 shows the response of the filtration rate of BSA solution to stepwise changes in the crossflow velocity during ultrafiltration experiments. The dynamically balanced filtration rate at stepwise increased velocity or stepwise decreased velocity tends to be in accord with that of ultrafiltration experiments conducted at constant crossflow velocity from the beginning of the process. Similar behavior is observed for silica sol. This indicates that the overall filtration characteristics of these gel-cakes are not influenced by the history of the shear stress acting on the gel-cake surface.

Figure 5 shows the effects of the mean diameter d_p of silica sol on the filtration rate. For dead-end ultrafiltration ($u_b=0$), the slope of $d\theta/dv$ versus v decreases and hence the filtration rate increases with d_p. For crossflow ultrafiltration, however, larger solute size does not necessarily lead to a higher filtration rate. For example, in the case where $d_p=48.3$ nm, a less pronounced effect is observed as shown in the figure, probably because gel-cake is hardly swept away. A possible explanation is that a large particle is not easily swept away by the small crossflow velocity ($u_b=1.9$ cm/s) although a increase in particle size causes a decrease in the specific filtration resistance of the gel-cake. Therefore, the relationship between the dynamically balanced filtration rate and the size of the solute is very complicated and is profoundly influenced by the crossflow velocity.

In **Fig. 6**, the effects of the transmembrane pressure p on the filtration rate are shown for BSA solution. The slope of $d\theta/dv$ versus v for dead-end ultrafiltration decreases slightly with increasing pressure. This can be explained by considering that the specific filtration resistance increases considerably with the pressure since the gel-cake of BSA is highly compressible.[10,11] The filtration rate in crossflow ultrafiltration also tends to increase slightly with increasing pressure.

It is difficult to determine the dynamically balanced filtration rate accurately on the basis of Fig. 6 because the filtration rate decreases gradually with v. The following analysis has been developed for determining the dynamically balanced filtration rate in crossflow ultrafiltration more accurately on the basis of the experimental results. The dead-end ultrafiltration rate q and the crossflow ultrafiltration rate q_c can be written as

$$\frac{1}{q}=\frac{d\theta}{dv}=\frac{\mu}{p}(R_g+R_m)=\frac{2}{K}v+\frac{\mu}{p}R_m \qquad (1)$$

$$\frac{1}{q_c}=\left(\frac{d\theta}{dv}\right)_c=\frac{\mu}{p}(R_{g\cdot c}+R_m) \qquad (2)$$

where μ is the viscosity of the permeate, R_m the hydraulic resistance of the membrane, K the Ruth coefficient of constant-pressure filtration,[19,20] and R_g

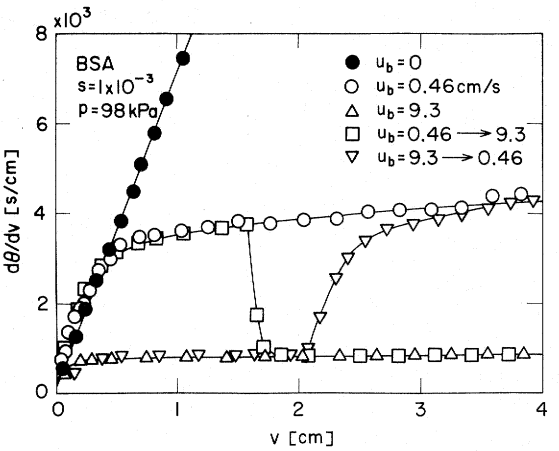

Fig. 4. Effects of stepwise changes in crossflow velocity on filtration rare

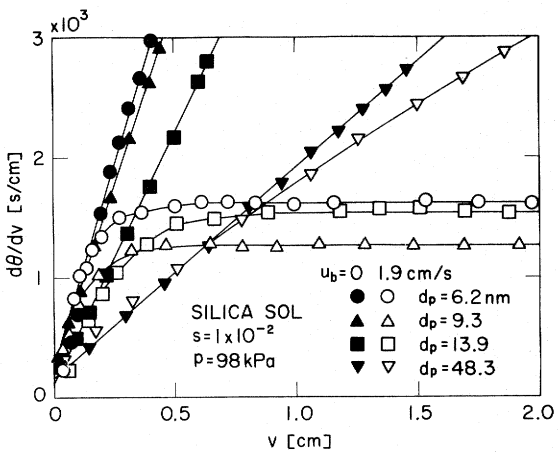

Fig. 5. Effects of mean diameter of silica sol on filtration rate

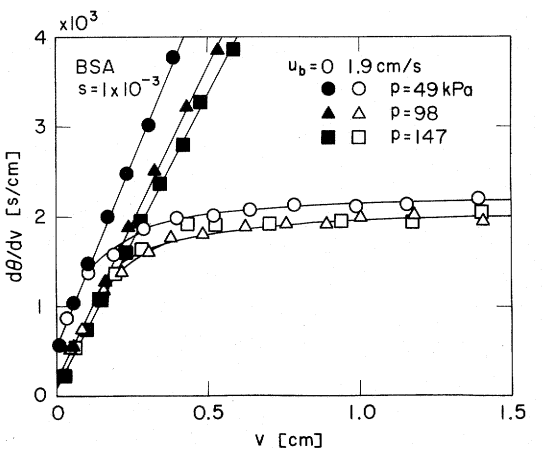

Fig. 6. Effects of filtration pressure on filtration rate

and $R_{g\cdot c}$ are the hydraulic resistance of the gel-cake for dead-end ultrafiltration and crossflow ultrafiltration respectively. Defining the crossflow filtration rate coefficient j_c[13] as the ratio of R_g to $R_{g\cdot c}$ and combining Eq. (1) with Eq. (2), q_c can be written as

$$\frac{1}{q_c}=\frac{1}{j_c}\left(\frac{1}{q}-\frac{\mu}{p}R_m\right)+\frac{\mu}{p}R_m=\frac{2}{j_cK}v+\frac{\mu}{p}R_m \qquad (3)$$

In **Fig. 7**, j_c versus v is illustrated on the basis of the experimental results in Fig. 6. It is apparent from the figure that j_c can be empirically related to v in the form

$$\left.\begin{aligned} j_c &= 1 && v \leqq v_t \\ j_c &= 1 + k(v - v_t) && v \geqq v_t \end{aligned}\right\} \qquad (4)$$

where k is an empirical constant which represents a measure of the crossflow effect, and v_t is the value of v below which the crossflow filtration rate coincides with the dead-end filtration rate. Substituting Eq. (4) into Eq. (3) and infinity into v, the dynamically balanced filtration rate q_e in crossflow ultrafiltration can be calculated by using the values of k and K. The flow rate q_e is plotted against the filtration pressure p in **Fig. 8**. Since q_e is relatively insensitive to pressure, high operating pressure is not required in the ultrafiltration process.

Figure 9 shows the filtration rates of BSA solution at different values of the bulk-stream concentration s. For dead-end ultrafiltration, the slope of $d\theta/dv$ versus v increases with s as suggested by Eq. (1) since K decreases with s. For crossflow ultrafiltration, the larger s becomes the smaller is the filtration rate. This can be explained by considering that the solutes are not easily swept away since the number of solutes accumulating on the gel-cake surface per unit time increases in the case of a large value of s. The logarithmic plot of q_e vs. s shows a linear relationship, as illustrated in Fig. 8.

2.2 Crossflow ultrafiltration model

A number of models have been proposed to explain the mechanism of crossflow ultrafiltration. Some of them are the gel polarization model,[2,9,17,18,25] the osmotic pressure model,[7,27,28] and the boundary-layer resistance model,[15,26] all of which are based on the well-known phenomenon of concentration polarization[8] whereby the convective transport of retained species to the membrane surface by the solvent is just equal to the diffusive transport of the solute from the membrane at steady state. We will provide further insight into the mechanism of crossflow ultrafiltration on the basis of the following experimental results. It was shown that the time variation of the filtration rate of crossflow ultrafiltration coincides with that of dead-end ultrafiltration until the filtration rate drops to a certain value, and that the flux decline can be significantly limited in dead-end upward ultrafiltration, in which the filtrate flow is opposite in direction to gravity.[6] To explain these observations, it seems appropriate to regard the gel-cake formed on the membrane as the structural assemblage of the "particulate" solutes. We have assumed that the flux of particles toward the gel-cake surface is counterbalanced at steady state by that of particles swept away from the gel-cake surface by the shear force induced by the tangentially flowing feed solution, on

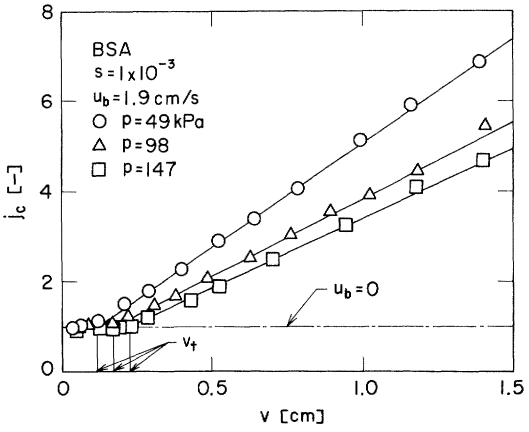

Fig. 7. Relation between j_c and v

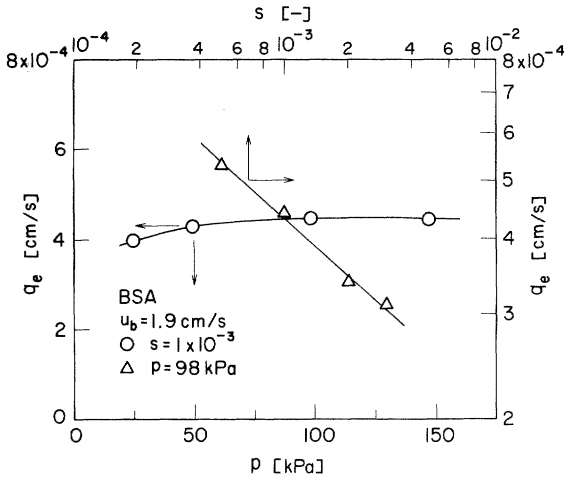

Fig. 8. Effects of filtration pressure and solute concentration on dynamically balanced filtration rate

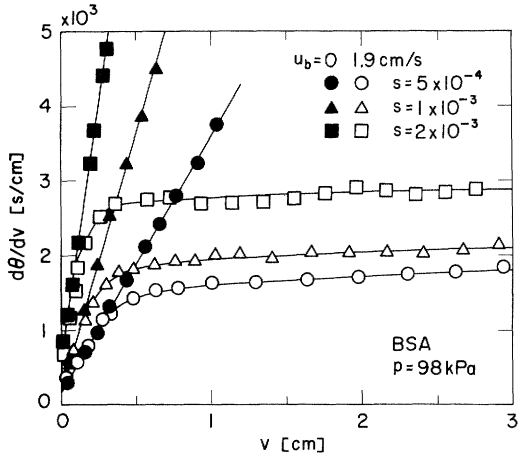

Fig. 9. Effects of solute concentration on filtration rate

the basis of the scour model[4,5] which has been applied to the analysis of crossflow microfiltration of suspensions. The overall material balance in dead-end ultrafiltration can be written as

$$w = \frac{\rho s}{1 - ms} v \qquad (5)$$

Differentiating Eq. (5) with respect to the filtration time θ and replacing the filtration rate by the dynamically balanced filtration rate q_e in crossflow ultrafiltration, the flux $q_{w\cdot e}$ of the solutes toward the gel-cake surface at steady state is given by

$$q_{w\cdot e}=\left(\frac{dw}{d\theta}\right)_e=\frac{\rho s}{1-ms}\left(\frac{dv}{d\theta}\right)_e=\frac{\rho s}{1-ms}q_e \qquad (6)$$

where w is the mass of solutes in gel-cake per unit membrane area, ρ the density of permeate, and m is the mass ratio of wet to dry gel-cake. In the case of a dilute solution where $(1-ms)$ is approximately unity, Eq. (6) reduces to

$$q_{w\cdot e}=\rho s q_e \qquad (7)$$

On the basis of the generalized equation of O'Brien and Rindlaub[16] derived from DuBoys' equation[3] for the motion of a sediment-laden stream over a layer of settled sediment, the flux $q'_{w\cdot e}$ of solutes to be swept away from the gel-cake surface can be given as a power function of the shear stress acting on the gel-cake surface by

$$q'_{w\cdot e}=a_1\tau_w^b \qquad (8)$$

where a_1 and b are empirical constants that depend on the characteristics of the gel-cake. Since $q'_{w\cdot e}$ is balanced by $q_{w\cdot e}$ at steady state, q_e may be found by combining Eq. (7) with Eq. (8). It is probable that the structure near the gel-cake surface becomes loose with increasing s as anticipated in modern filtration theory[22] since the number of particles approaching the gel-cake surface per unit time increases with s. Considering that such a loose gel-cake is easily swept away, q_e may be modified as

$$q_e=a_2 s^{-d}\tau_w^b \qquad (9)$$

This equation indicates that a logarithmic plot of q_e versus s shows a linear relationship, and that q_e is unaffected by p, in accord with the observed tendencies shown in Fig. 8. Equation (9) reduces to the equation presented by Fane *et al.*[4,5] by putting b as unity. They considered that in general τ_w is represented by a power function of u_b, and that τ_w is directly proportional to u_b under laminar flow conditions.

2.3 Comparison of upward and downward ultrafiltration of crossflow type

The effects of the crossflow velocity u_b on the dynamically balanced filtration rate q_e for both upward and downward ultrafiltration are shown as logarithmic plots of q_e versus τ_w in **Fig. 10**. It may be postulated that the permeation flux through the gel-cake is negligible compared with the flux of crossflow, and that the thickness of the gel-cake is negligibly small compared with the thickness h of the filter chamber.[10,11] In this study, as a satisfactory approximation the shear stress at the membrane

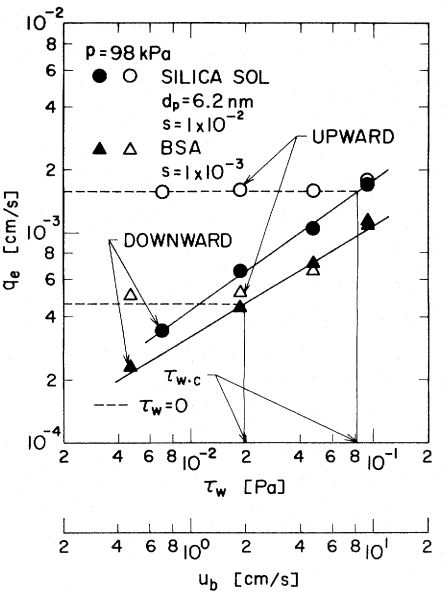

Fig. 10. Effects of shear stress at gel-cake surface on dynamically balanced filtration rate in both upward and downward ultrafiltration

surface of the laminar flow in a channel with two parallel flat walls may be employed as

$$\tau_w=6\mu_s u_b/h \qquad (10)$$

where μ_s is the viscosity of the solution. The plots for crossflow downward ultrafiltration of silica sol and BSA solutions are substantially linear in accordance with Eq. (9). On the other hand, in crossflow upward ultrafiltration, q_e becomes invariant at values of τ_w, below $\tau_{w\cdot c}$, which is the critical shear stress. This constant value coincides with that of dead-end upward ultrafiltration where τ_w equals zero. This means that the quantity of gel-cake that can be supported on the membrane in upward ultrafiltration under conditions below $\tau_{w\cdot c}$ is constant, even if crossflow is added. The flow rate q_e in crossflow upward ultrafiltration is in accord with that in crossflow downward ultrafiltration when operated above $\tau_{w\cdot c}$. Thus dead-end upward ultrafiltration is more effective than crossflow downward ultrafiltration below $\tau_{w\cdot c}$, whereas above $\tau_{w\cdot c}$ crossflow filtration is more efficient for flux enhancement than dead-end upward filtration. It should be also noted that in such ultrafiltration process applications as tubular, spiral, hollow-fiber, and plate-and-frame modules,[1] the effects of upward or inclined ultrafiltration[6] must be taken into consideration in filtration tests conducted under conditions below $\tau_{w\cdot c}$.

Conclusions

The characteristics of crossflow ultrafiltration were examined by using proteinaceous and colloidal solutions. In the initial stage of crossflow ultrafiltration the time variations of the filtration rate were in

accord with those of dead-end ultrafiltration in the same manner as in the case of microfiltration. However, the gel-cake of ultrafiltration was easily swept away by a small crossflow velocity compared with microfiltration. The effects of the crossflow velocity u_b (the shear stress τ_w), the filtration pressure p, and the solute concentration s on the measured filtration characteristics were well explained by considering that the particulate solutes which are carried to the gel-cake surface are swept away by the shear force induced by tangential flow. In addition, the difference was examined between upward and downward ultrafiltration of the crossflow type. The effective range for dead-end upward ultrafiltration and that for conventional crossflow ultrafiltration were shown by introducing the concept of the critical shear stress.

Acknowledgement

The authors wish to express their sincere appreciation to Nissan Chemical Ind. for supply of silica sol.

Nomenclature

a_1	=	empirical constant in Eq. (8)	$[kg^{-b}m^{b+1}s^{2b-1}]$
a_2	=	empirical constant in Eq. (9)	$[kg^{-b}m^{b+1}s^{2b-1}]$
b	=	empirical constant in Eq. (8)	[—]
d	=	empirical constant in Eq. (9)	[—]
d_p	=	mean diameter of solute	[m]
h	=	thickness of filter chamber	[m]
j_c	=	crossflow filtration rate coefficient	[—]
K	=	Ruth coefficient of constant-pressure filtration	$[m^2/s]$
k	=	empirical constant in Eq. (4)	$[m^{-1}]$
L	=	length of filter chamber	[m]
m	=	ratio of wet to dry gel-cake mass	[—]
p	=	applied filtration pressure	[Pa]
q	=	filtration rate in dead-end ultrafiltration	[m/s]
q_c	=	filtration rate in crossflow ultrafiltration	[m/s]
q_e	=	dynamically balanced filtration rate	[m/s]
$q_{w\cdot e}$	=	flux of solute toward gel-cake surface at steady state	[m/s]
$q'_{w\cdot e}$	=	flux of solute to be swept away from gel-cake surface at steady state	[m/s]
R_g	=	hydraulic resistance of gel-cake for dead-end ultrafiltration	$[m^{-1}]$
$R_{g\cdot c}$	=	hydraulic resistance of gel-cake for crossflow ultrafiltration	$[m^{-1}]$
R_m	=	hydraulic resistance of membrane	$[m^{-1}]$
s	=	mass fraction of solute in solution	[—]
u_b	=	crossflow velocity	[m/s]
v	=	filtrate volume per unit membrane area	$[m^3/m^2]$
v_t	=	filtrate volume per unit membrane area defined in Eq. (4)	$[m^3/m^2]$
w	=	mass of solute in gel-cake per unit membrane area	$[kg/m^2]$
θ	=	filtration time	[s]
μ	=	viscosity of permeate	[Pa·s]
μ_s	=	viscosity of solution	[Pa·s]
ρ	=	density of permeate	$[kg/m^3]$
τ_w	=	shear stress at membrane surface	[Pa]
$\tau_{w\cdot c}$	=	critical shear stress at membrane surface	[Pa]

〈Subscript〉

t	=	transition point

Literature Cited

1) Belfort, G.: *J. Memb. Sci.*, **35**, 245 (1988).
2) Doshi, M. R. and D. R. Trettin: *Ind. Eng. Chem. Fundam.*, **20**, 221 (1981).
3) DuBoys, M. P.: *Annales de Ponts et Chaussés*, Ser. 5, **18**, 141 (1879).
4) Fane, A. G., C. J. D. Fell and M. T. Nor: *Inst. Chem. Engrs. Symp. Ser.*, **73**, C1 (1982).
5) Fane, A. G.: "Progress in Filtration and Separation 4, Ultrafiltration: Factors Influencing Flux and Rejection" (ed. by R. J. Wakeman), p. 145, Elsevier, Netherlands (1986).
6) Iritani, E., T. Watanabe and T. Murase: *Kagaku Kogaku Ronbunshu*, **17**, 206 (1991).
7) Jonsson, G.: *Desalination*, **51**, 61 (1984).
8) Kimura, S. and S. Sourirajan: *AIChE J.*, **13**, 497 (1967).
9) Michaels, A. S.: *Chem. Eng. Progress*, **64**, 31 (1968).
10) Murase, T., E. Iritani, S. Nakatsuka and M. Shirato: *Kagaku Kogaku Ronbunshu*, **14**, 241 (1988).
11) Murase, T., E. Irigani, S. Nakatsuka, H. Aoki and M. Shirato: Preprints of Gifu Meeting of The Soc. of Chem. Engrs., Japan, p. 148 (1988).
12) Murase, T., E. Iritani, P. Chidphong and K. Kano: Preprints of the 54th Annual Meeting of The Soc. of Chem. Engrs., Japan, p. 387, Kobe (1989).
13) Murase, T., E. Iritani, P. Chidphong, K. Kano, K. Atsumi and M. Shirato: *Kagaku Kogaku Ronbunshu*, **15**, 630 (1989).
14) Murase, T., E. Iritani and P. Chidphong: Preprints of the 55th Annual Meeting of The Soc. of Chem. Engrs., Japan, p. 88, Nagoya (1990).
15) Nakao, S., J. G. Wijmans and C. A. Smolders: *J. Memb. Sci.*, **26**, 165 (1986).
16) O'Brien, M. P. and B. D. Rinḍlaub: *Transactions, Amer. Geophy. Union*, **15**, 593 (1934).
17) Porter, M. C.: *Ind. Eng. Chem. Product Res. Develop.*, **11**, 234 (1972).
18) Probstein, R. F., J. S. Shen and W. F. Leung: *Desalination*, **24**, 1 (1978).
19) Ruth, B. F.: *Ind. Eng. Chem.*, **27**, 708 (1935).
20) Ruth, B. F.: *Ind. Eng. Chem.*, **38**, 564 (1946).
21) Shirato, M. and S. Okamura: *Kagaku Kōgaku*, **20**, 678 (1956).
22) Shirato, M. and M. Sambuichi: *Kagaku Kōgaku*, **27**, 470 (1963).
23) Shirato, M., T. Murase, E. Iritani, F. M. Tiller and A. F. Alciatore: "Filtration (Principles and Practices), 6 Filtration in the Chemical Process Industry" (ed. by M. J. Matteson and C. Orr), p. 348, Marcel Dekker, Inc., New York (1987).
24) Tiller, F. M., C. S. Yeh and W. F. Leu: *Sep. Sci. Tech.*, **22**, 1037 (1987).
25) Trettin, D. R. and M. R. Doshi: *Ind. Eng. Chem. Fundam.*, **19**, 189 (1980).
26) van den Berg, G. B. and C. A. Smolders: *Filtration & Separation*, **25**, 115 (1988).
27) Vilker, V. L., C. K. Colton and K. A. Smith: *AIChE J.*, **27**, 637 (1981).
28) Wijmans, J. G., S. Nakao and C. A. Smolders: *J. Memb. Sci.*, **20**, 115 (1984).

(Presented at the 55th Annual Meeting of The Society of Chemical Engineers, Japan, at Nagoya, April, 1990.)